AIP Advances

Study of oxidation processes in Mo/Be multilayers

Cite as: AIP Advances 8, 075202 (2018); https://doi.org/10.1063/1.5007008
Submitted: 29 September 2017 • Accepted: 04 June 2018 • Published Online: 02 July 2018

A. N. Nechay, N. I. Chkhalo, M. N. Drozdov, et al.

ARTICLES YOU MAY BE INTERESTED IN

IMD—Software for modeling the optical properties of multilayer films
Computers in Physics 12, 360 (1998); https://doi.org/10.1063/1.168689

Spectral tailoring of nanoscale EUV and soft x-ray multilayer optics
Applied Physics Reviews 4, 011104 (2017); https://doi.org/10.1063/1.4978290

Review Article: Stress in thin films and coatings: Current status, challenges, and prospects
Journal of Vacuum Science & Technology A 36, 020801 (2018); https://doi.org/10.1116/1.5011790

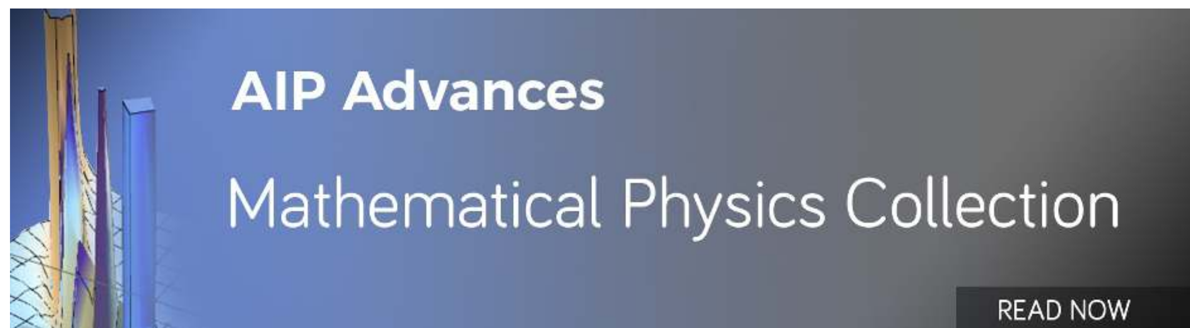

© 2018 Author(s).

Study of oxidation processes in Mo/Be multilayers

A. N. Nechay,[1,a] N. I. Chkhalo,[1] M. N. Drozdov,[1] S. A. Garakhin,[1]
D. E. Pariev,[1] V. N. Polkovnikov,[1] N. N. Salashchenko,[1] M. V. Svechnikov,[1]
Yu. A. Vainer,[1] E. Meltchakov,[2] and F. Delmotte[2]
[1]*Institute for Physics of Microstructures of Russian Academy of Sciences, Akademicheskaya St., 7, Nizhny Novgorod 603087, Russia*
[2]*Laboratoire Charles Fabry, Institut d'Optique Graduate School, CNRS, Université Paris-Saclay, 2 Avenue Augustin Fresnel, 91127 Palaiseau Cedex, France*

(Received 29 September 2017; accepted 4 June 2018; published online 2 July 2018)

The results of an investigation on oxidation processes in Mo/Be multilayer nanofilms are presented. The films annealed both in ambient atmosphere and in vacuum. The extreme ultraviolet (EUV) and X-ray reflectivity of the samples at 11.34 and at 0.154 nm respectively were measured before and after the treatment. No noticeable changes in film thicknesses and boundaries were observed during the annealing at temperatures up to 300°C. An oxidation mechanism of the nanofilms Mo/Be is established and the activation energy of the oxidation process is estimated to be 38 kJ/mol. To determine an absolute quantity of oxygen in the oxidized layers, a simple technique based on the EUV reflectivity data is proposed, and the range of its applicability is subsequently analysed. © *2018 Author(s). All article content, except where otherwise noted, is licensed under a Creative Commons Attribution (CC BY) license (http://creativecommons.org/licenses/by/4.0/).* https://doi.org/10.1063/1.5007008

INTRODUCTION

New projects for solar corona imaging impose new requirements for material combinations used in multilayer mirror (MLM) designs such as to provide both high reflectance and a good spectral selectivity in the EUV range. It was shown in Ref. 1 that Be-based MLMs meet these requirements to the greatest extent due to the unique combination of optical constants of Be. In particular, MLMs composed of Mo/Be have better spectral selectivity than traditional Mo/Si MLMs[2] and are more suitable for detecting emission lines of iron ions Fe(XX), Fe(XXI), Fe(XXIII) in the vicinity of 13 nm. The Mo/Be multilayered system was previously considered as one of the candidates for EUV photolithography at the wavelength of 11.3 nm.[3,4] Subsequently, the alternative wavelength of 13.5 nm was chosen, and the preference was given to Mo/Si MLM designs since these have the highest reflectivity (up to 70.15%) at this wavelength.[5] Presently, however, the interest in Mo/Be MLMs is rising again owing to a possible selection of shorter wavelength for the next generation of EUV lithography[6] instead of the previously considered 6x nm project. For instance, a nanolithography station with a working wavelength 11.2 - 11.3 nm is currently being developed.[7]

Moreover, the Mo/Be may be of interest for "classical" EUV lithography. First, due to a lower absorption of Be as compared with Si, Be-containing free-standing multilayer films, in particular Mo/Be, can be used as cut-off filters and "pellicles" to protect photolithographic masks from contamination.[8] Secondly, it was recently shown that tri-material Mo/Be/Si MLMs routinely provide a peak reflectivity in the 13.5 nm region of more than 71%, with record values of about 72%.[9] Taking into account the multi-mirror nature of modern lithography projection schemes, this can result in a significant economic benefit for mass production of chips.

[a]nechay@ipm.sci-nnov.ru

 © Author(s) 2018

For both space and lithography applications, a good temporal stability of the multilayer characteristics is extremely important, as well as a resistance to heating for the coatings operating in an elevated temperature environment or exposed to a high radiation flux. In addition to the resistance of MLMs to heating, there is a practical interest to the resistance to Mo/Be MLMs to oxidation processes, even under high vacuum conditions. To assess the long-term stability of the films in the work, the activation energy of the oxidation processes was determined. To accelerate the oxidation process, annealing was carried out in air. To separate the effects associated with oxidation and interlayer diffusion, identical samples were annealed in air and in vacuum. In the paper the questions of samples preparation, characterization and annealing are given in details, followed by the stability evaluations.

SAMPLE PREPARATION AND EXPERIMENTAL METHODS

The Mo/Be multilayer with 110 bi-layers was deposited on a 100 mm silicon wafer. The wafer was subsequently diced into 20×20 mm^2 samples. Deposition was carried out using DC magnetron sputtering with the following process parameters: the residual vacuum pressure is 5×10^{-5} Pa, the working gas (Ar) pressure is 7×10^{-2} Pa, the current through the Mo target is 600 mA and the voltage is 270 V, whereas 900 mA and 300 V were used for the Be target respectively. More details on the deposition process can be found elsewhere.[1]

The film thicknesses, the profile of transition layers at the boundaries and film densities in the deposited MLMs were retrieved from a joint analysis of grazing incidence X-ray reflectivity (GIXR) data (at 0.154 nm) and a near-normal incidence reflectivity of samples measured at 11.34 nm. The so-called "extended" model based on X-ray reflectivity data[10] was used for the reconstruction of MLM parameters. The main feature of this approach, in contrast to traditional models,[11] is the representation of a transition region profile in the form of a linear combination of the following functions: error function, linear, exponential, sinusoidal, hyper-tangent and step function. The coefficients for the corresponding functions are treated as fitting parameters. This approach allows one to account for various mechanisms of transition layer formation. For example, the annealing of a particular MLM can cause drastic changes in the boundary profile, which will manifest itself as changes in the corresponding function coefficients. One of the advantages of this model is that it is capable of adequately describing the stoichiometric component within the transition layer (for instance, the formation of chemical compounds) due to the introduction of the step function. More details on how one can account for the oxidation of the upper layers will be described later.

The measurements in the EUV spectral range were carried out using a reflectometer equipped with high resolution grazing incidence spectrometer-monochromator and dismountable X-ray tube.[12] Most of the measurements were performed at the wavelength of 11.34 nm, which corresponds to the maximum of the K-line emission from the Be target.

Time-of-flight (TOF) secondary ion mass spectrometry (SIMS) was used as an auxiliary research technique. The elemental analysis of nanofilms was carried out using the TOF.SIMS-5 installation by IONTOF (Münster, Germany) with a TOF mass analyzer. This system uses a pulsed mode of operation, which allows for the separation of effects from two ion beams for analysis and etching. The etching is produced by O_2^+ or Cs^+ ions with energies from 0.5 to 2 keV, with an angle of incidence on the surface of 45°; the beam current is on the order of a few hundred nanoamps. A typical size of the etching beam raster is from 200×200 μm^2 to 500×500 μm^2. O_2^+ ions were used for the analysis of metal distribution, and Cs^+ ions were used for oxygen profiling. Etching by different ions was performed at different points on the sample surface.

For the analysis, the probing ions from heavy Bi^+ elements with an energy of 25 keV were used. The beam current of these Bi ions did not exceed 1 pA, and the pulse duration was 1 ns. The technique is described in more detail elsewhere.[13]

One part of each sample was annealed in a muffle furnace in air atmosphere. After annealing, the multilayers were taken out and cooled down to ambient temperature. Another part of each sample was annealed in vacuum using a special furnace pumped to a pressure of 1×10^{-4} Pa. All samples were annealed for a preset time at a given temperature and subsequently cooled down inside the furnace.

EXPERIMENTAL RESULTS

GIXR measurements

Figure 1 shows the measured and fitted angular reflectivity dependencies for the as-prepared Mo/Be sample at wavelengths of 0.154 and 11.34 nm. The number of periods is 110 and the top layer is Be. Note the different vertical scales for both. The MLM parameters obtained by the fitting algorithm are as follows: the thickness of the Be layer is 3.23 nm, the thickness of the Mo layer is 2.79 nm; their densities are assumed equal to the tabulated values: ρ_{Be} = 1.848 g/cm^3 and ρ_{Mo} = 10.22 g/cm^3; the period drift from the top to the bottom of the MLM is estimated to be 0.12 nm (approximately 2% of the period). The average roughness of the Be-on-Mo interface is about 0.35 nm and that of the Mo-on-Be is 0.9 nm. The boundaries are described well by a combination of an error function, an exponential function and a sinusoidal function, i.e. $A^*\mathrm{erf}(z)+B^*\exp(z)+C^*\sin(z)$. The superposition of the error function, the exponential and the sine functions imply that the profile of the interlayer region has no strong leaps or fractures, but its "tails" to each layer are longer that for conventional error function. This is the reason for the less rapid decrease of the Bragg peaks in Fig. 1 (left) to high grazing angles of the probing beam.

The Mo/Be MLMs were annealed in air atmosphere at temperatures of 200, 250, 300, 350, 400 and 450°C. Figure 2 shows GIXR curves corresponding to annealed samples at 300, 350 and 400°C during 0, 2 and 8 hours. Annealing up to 350°C is observed to not practically affect the positions of the diffraction peaks. However, at higher temperatures, the positions of the Bragg peaks are shifted (less than 0.5%), implying that the multilayer period has contracted. Another interesting feature from the reflectivity curves is in between the region of total external reflection and the first Bragg peak (angular region around 0.5°). These changes become more significant with increasing temperature and/or duration of the anneal in air. This feature is not observed in the GIXR curves of Mo/Be annealed in vacuum at 350°C (see Fig. 3) for 0, 2.5 and 7 hours. It can therefore be concluded that the above mentioned changes are due to surface oxidization processes.

To reconstruct the multilayer structure, the "extended" model was revised by adding further variable parameters including thicknesses and layer densities, the shape and width of the inter-layer transition regions estimating the interfacial roughness and inter-diffusion of the multilayer materials. While constructing the oxidized layer model, the following assumptions were used based on SIMS data. At "low" annealing temperatures (<250°C), only the top Be layer is oxidized into BeO (with a density 3.01 g/cm^3) as this is the case of a single Be film stored in ambient conditions for several months. At "high" annealing temperatures (>350°C), the two outermost layers (i.e. the last deposited period) are fully oxidized. Moreover, an intermixing occurs between the oxidized layers of Be and Mo. The layers of penultimate period are partly oxidized without intermixing. In the intermediate temperature range (250–350°C), both scenarios were deemed possible. More details on the results of SIMS measurements will be given in the next section.

Figure 4 shows the results of the reflectivity measurements and the corresponding fits for the Mo/Be sample annealed in air at 400°C in air for 4 hours. In the proposed model, the last two periods

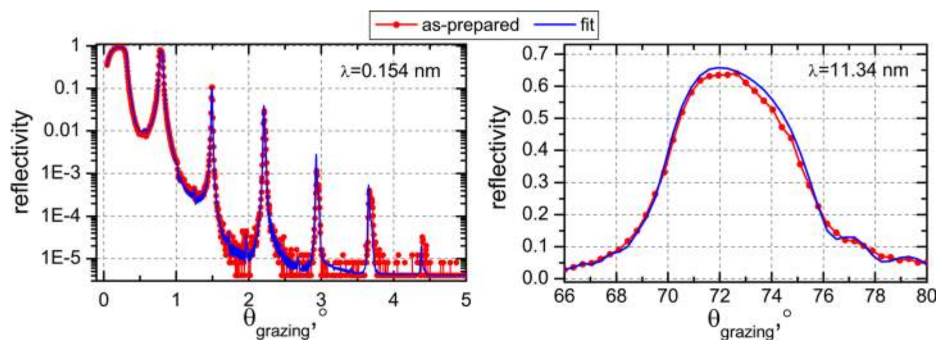

FIG. 1. X-ray (left) and EUV (right) reflectivity curves as a function of incident angle of as-prepared Mo/Be multilayer. Red line + dots – measurement, blue line – model fit.

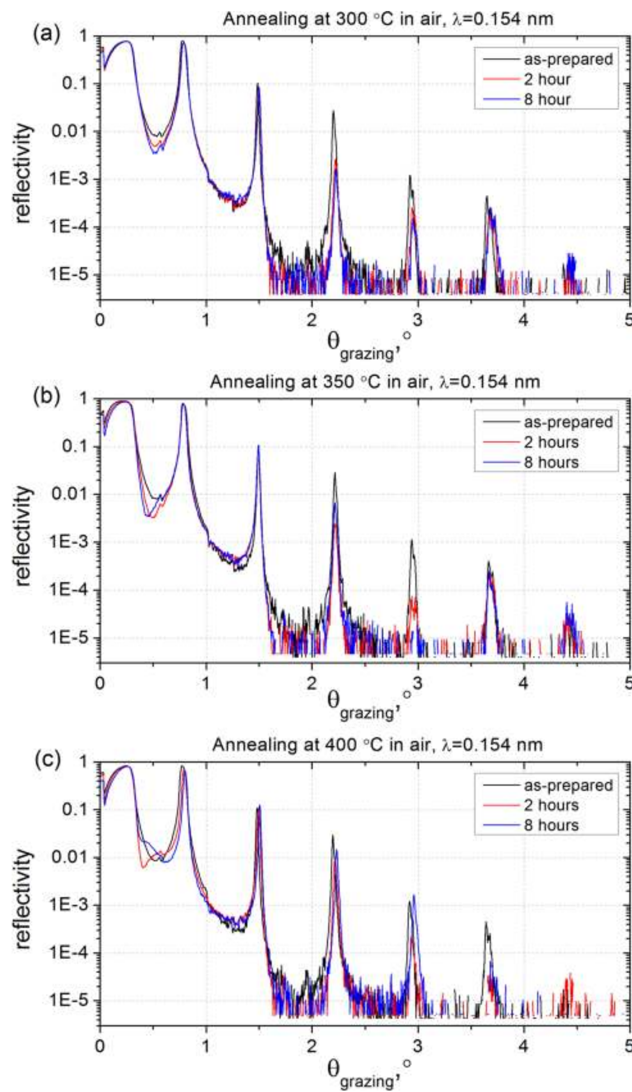

FIG. 2. GIXR curves of Mo/Be MLMs before and after annealing at different temperatures in air: (a) 300°C, (b) 350°C, (c) 400°C. Before annealing – black curve, annealing time 2 hours – red curve and 8 hours – blue curve.

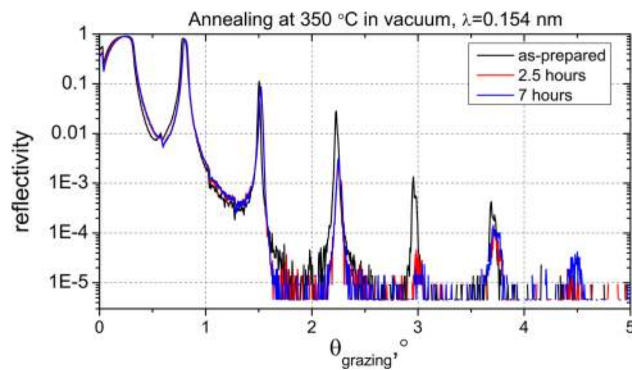

FIG. 3. GIXR curves of Mo/Be MLMs before and after annealing at 350°C in vacuum: before annealing – black curve, annealing time 2.5 hours – red curve and 7 hours – blue curve.

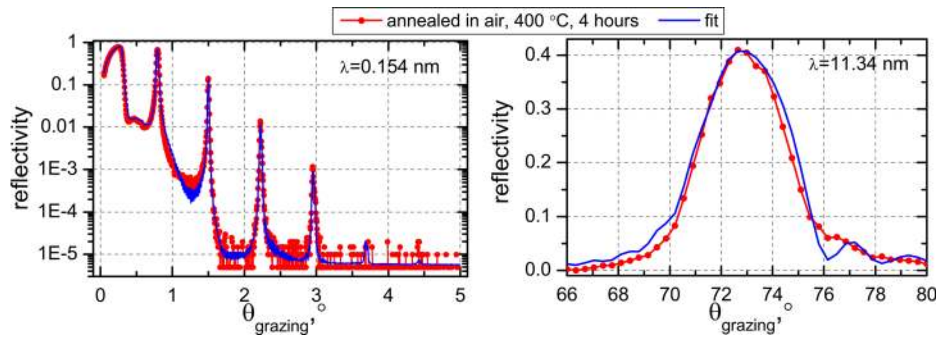

FIG. 4. GIXR and EUV reflectivity curves of the Mo/Be sample annealed in air at 400°C for 4 hours. Red – measurement, blue – model fit.

(i.e. four upper layers) are fully oxidized and intermixing of the top bi-layer materials lead to the formation of a $Mo_xBe_yO_z$ film.

It can be concluded that the annealing of Mo/Be at temperatures higher than 350°C results in essential structural changes deeply within the nanofilms, which are caused by inter-diffusion. These changes are clearly visible on the GIXR curves. The statement concerning diffusion is supported by the fact that the profile of the interface region changes from the superposition of the sinusoidal, exponential and error functions to a linear function. The linear function of the interfaces is characteristic of MLMs with strong inter-diffusion, for instance, Ni/C[14] and La/B_4C (La/B)[15–17] multilayers. In contrast, annealing at temperatures below 300°C results in small changes to the thicknesses and densities of layers as well as the transitional regions; furthermore, the reflectivity drop is mainly caused by surface oxidation (for annealing in air). The depth of the oxidized surface region formed as a result of annealing in air atmosphere depends on both temperature and annealing time.

Reflectometry at 11.34 nm

EUV reflectivity was measured at 11.34 nm for samples annealed in air and in vacuum at temperatures from 200 to 450°C in 50°C increments. The evolution of the angular dependence of the reflectance is illustrated in Fig. 5 for the sample annealed at 400°C in air atmosphere for 2 and 8 hours. After 8 hours, the change in the Bragg peak position corresponds to a decrease in period of about 0.03 nm, and indicates the beginning of a structural change in the sample. Significant changes are observed for the reflection coefficient magnitude: during annealing, the reflectance decreases by about 35%.

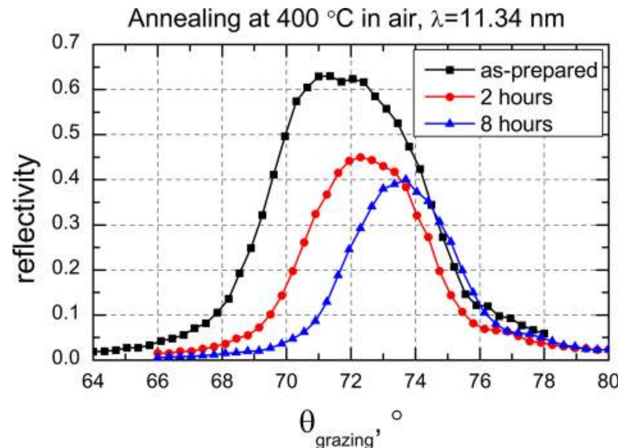

FIG. 5. The EUV reflectivity curves of Mo/Be samples annealed at 400°C in air, black – before annealing, red – annealed for 2 hours, and blue – after 8 hours of annealing.

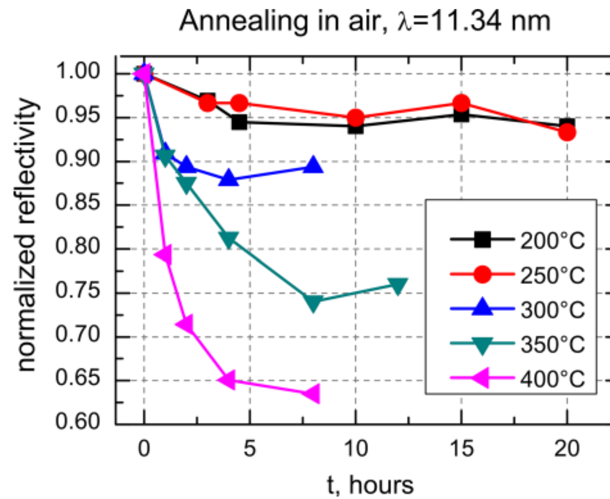

FIG. 6. The EUV peak reflectance (normalized) of Mo/Be MLMs as a function of the time and the temperature of annealing in air atmosphere.

Fig. 6 shows the EUV peak reflectance of Mo/Be multilayers (normalized to the reflectance of the as-prepared sample) as a function of the annealing time in air at different temperatures. The uncertainty on the reflectivity measurement is ±3%. It can be seen that for low annealing temperatures, the reflectance decreases only slightly, whereas for the higher temperatures, the loss in reflectance is much more significant. The rapid initial drop in the reflectance is followed by a more moderate reduction. The results of these measurements show that a significant degradation in reflectivity of more than 10%) for the Mo/Be MLMs occurs for annealing temperatures above 300°C in air. At lower temperatures, these MLMs can be stored in ambient atmosphere for a long period of time with no dramatic loss in performance.

The dependencies of EUV reflectance on time and annealing temperature in vacuum of Mo/Be MLMs are plotted in Fig. 7, where the peak reflectance is again normalized to the as-prepared sample. A stable response at annealing temperatures ≤300°C are measured within 3%. At temperatures above 350°C, the trend changes, so one can conclude that the mirror begins to degrade, which becomes imminent at temperatures above 400°C. A small shift in the Bragg peak positions in the GIXR curves

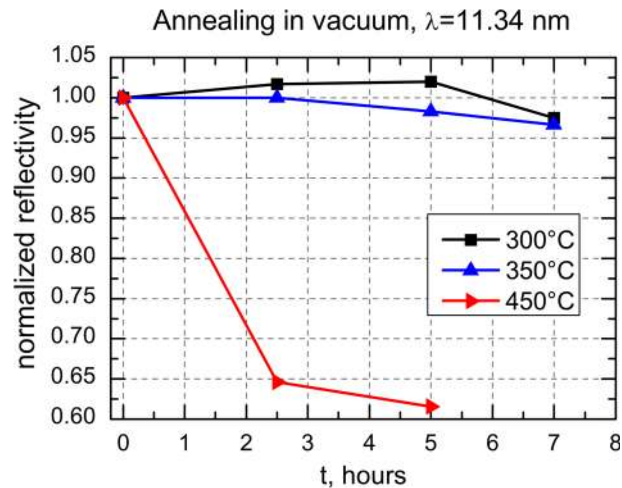

FIG. 7. The EUV peak reflectance (normalized) of Mo/Be MLMs as a function of the time and the temperature of annealing in vacuum.

of the Mo/Be samples annealed in vacuum at temperatures greater than 350°C was also observed (see Fig. 3).

Thus, it can be assumed that the layer densities and the interfacial roughness remain unchanged in the Mo/Be MLMs upon annealing in vacuum at temperatures up to 300°C. It can also be assumed that the degradation of EUV reflectivity annealed in air at temperatures up to 300°C is related to the oxidation of the near-surface layers in the nanofilms, which becomes less transparent to probing radiation. The critical temperature of 350°C results in a change in internal structure of the Mo/Be MLM. At higher temperatures, the degradation process appears to be fast.

TOF-SIMS measurements

The TOF-SIMS technique has become widely used for qualitative and, to some extent, quantitative elemental analysis of thin film and multilayer composition and distribution of elements from the surface down to deeper layers.[13,18,19] This technique was used to study the distribution profiles of the main elements (Mo, Be, O, C) within Mo/Be MLMs with a period of 6 nm. Figure 8 shows the oxygen profile in the near-surface layers (approximately the last 10 deposited periods of the stack) of as-deposited and annealed in air (350°C for 12 hours) samples. The recorded signal from oxygen ions (in terms of counts per second) is plotted as a function of depth, which is known from GIXR data.

The initial part of each curve is an artifact due to a delay in the beginning of the sputtering process. The plateau corresponds to a fully oxidized surface layer, and the concentration of oxygen atoms begins to decrease down to values representing the quantity of oxygen penetrating into the stack either during deposition or annealing. It can be estimated that the as-deposited sample has a partially oxidized region (approx. 3 nm thick) with variable oxide stoichiometry. The annealed sample, however, is characterized by a 12 nm thick fully oxidized region and a partially oxidized layer of about 3 nm. The changes in the oxygen profile were determined to be caused by annealing temperatures above 200°C.

As can be seen from Fig. 8, the modulation of the oxygen profile in the deeper layers of the annealed sample have a lower amplitude than the as-prepared sample, but the average oxygen content remains practically the same. This effect can be explained by a redistribution of oxygen within the stack. During the growth of the multilayer stack, the oxygen atoms are mainly absorbed in the Be layers. After annealing, they diffuse into neighboring layers. Such a redistribution of the oxygen content between Be and Mo layers can explain the small increase in the reflectance of the MLM (comparable to the measurement error) annealed in vacuum at 300°C (see Fig. 7).

The TOF-SIMS technique was also used to probe the Be and Mo contents in the MLMs and to study the effect of annealing on their respective distributions in the near-surface region of the

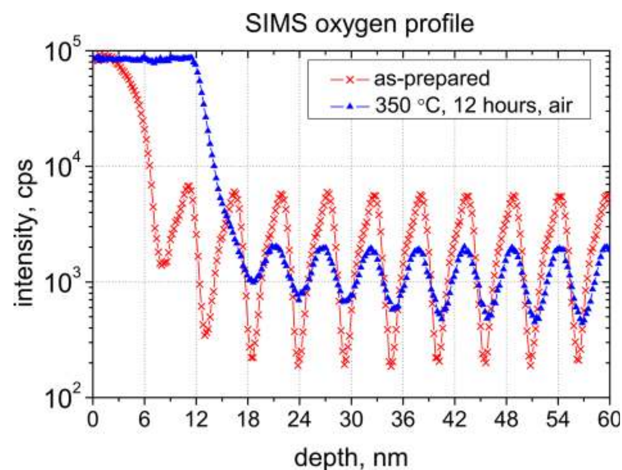

FIG. 8. The oxygen distribution in the near-surface layers of as-deposited (red crosses) and annealed at 350°C during 12 hours in air (blue triangles) Mo/Be samples.

structure. The measured Be and Mo depth profiles are plotted on Fig. 9 for (a) as-deposited samples and (b) samples annealed in air atmosphere at 350°C. The signals recorded from the two elements are normalized to their respective maxima. The observable modulation of Mo and Be in Fig. 9(a) is lower in first period due to surface effects, specific for SIMS technique, and not real. This is connected with the contamination of near-surface layers with other elements even in as-prepared sample. After few periods the modulation is diminishing due to roughness increase during etching process. A good contrast between the Be and Mo layers observed for the as-deposited sample is missing in the outermost layers of the annealed sample that is fully oxidized and intermixed. As a consequence, this region of the annealed MLM does not contribute to the constructive interference of the reflected light, and instead, absorbs a component of the radiation leading to the observed decrease in the EUV reflectance of the multilayers.

Determination of the quantity of oxygen in multilayer films

Different methods exist to determine the absolute quantity of oxygen in solids, which is not always a simple task, but these methods either do not reliably provide an acceptable accuracy (for instance, the total weight) or require a special (and rather expensive) piece of equipment (for example, the neutron activation analysis). Furthermore, large uncertainties are typically associated with the specificity of the surface layer.[20]

One of the most convenient and sensitive methods, in the opinion of the authors, is the measurement of absorption of EUV radiation by oxygen. By specifying the wavelength, it is possible to expand the dynamic range of the oxygen concentration measurements, and to detect both small and relatively large quantities of adsorbed oxygen. However, the absorption caused by oxidization can only be measured with thin free-standing films of a certain thickness. The fabrication of such films is a feasible but rather complicated process.[21] Therefore, to estimate the quantity of oxygen, the reflectance of the multilayers with an oxidized surface is proposed as a function of an "effective"

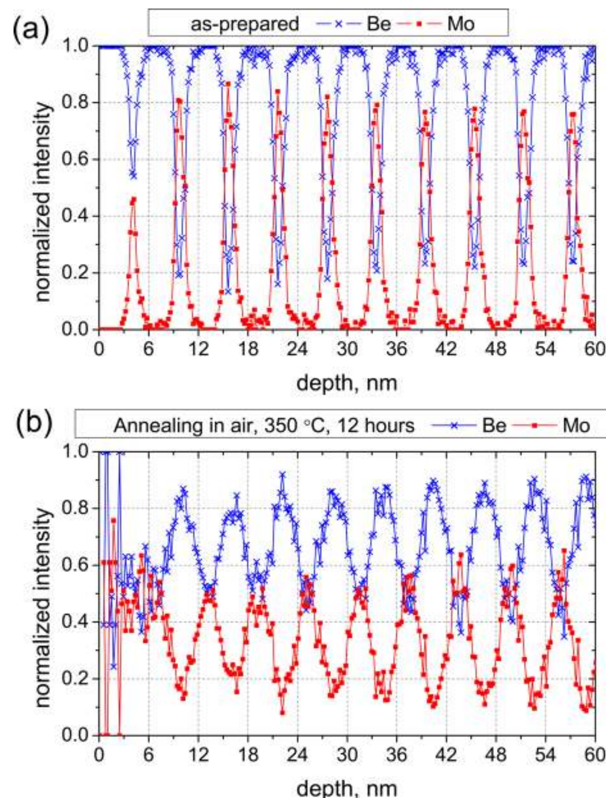

FIG. 9. The Be and Mo depth profiles in as-deposited (a) and annealed (b) in air at 350 °C during 12 hours Mo/Be multilayers.

thickness of the surface oxide layer. This method is quite simple and only requires measuring the EUV reflectivity.

This approach is deemed acceptable due to the negligible dependence of the atomic absorption and scattering processes in the X-ray range on the presence of chemical bonds in solids. However, assuming *a priori* that the decrease in reflectivity is solely caused by oxidation can limit the reliability of this method. In practice, any change in the state of the boundaries between the layers and, to a lesser extent, in the densities of the materials can result in significant variation in the multilayer reflectance.

To define the limits of applicability of the proposed method, the analysis of GIXR and EUV reflectivity data were used for as-deposited and annealed samples as well as the TOF-SIMS results. First, it can be concluded that no significant structural changes occurred in the bulk Mo/Be multilayers annealed up to temperatures as high as 300°C, which could affect the reflectance of the MLMs in the EUV range. Second, from SIMS measurements, only the outermost layers were susceptible to oxidation and, thus, the formation of the surface oxide film absorbing the probing radiation is, to a greater extent, responsible for the reduction of the EUV peak reflectance of MLMs.

In the "effective" oxide film model for the MLM surface, the intensity of radiation transmitted through the sample is given by:

$$J = J_0 \times \exp(-{}^{\mu}\!/_{\rho} \times 2m) \quad (1)$$

where J and J_0 are the intensities of the transmitted and incident radiation respectively, m is the mass of the absorbing material per unit area (g/cm^2), $2m$ corresponds to the double pass of radiation through the oxide film, and μ/ρ is the mass attenuation coefficient. For oxygen, this value is 5.66×10^4 cm^2/g at wavelength of 11.34 nm.[22]

In accordance with Eq. (1), the absolute quantity of oxygen in the oxide layer (in g/cm^2) was calculated as a function of the annealing time and temperature. The results of these calculations are shown in Fig. 10. At all annealing temperatures, the oxygen concentration was found to rise rapidly during the first hour of annealing, followed by a slower increase in oxygen content with a tendency to saturate. For instance, upon annealing at temperature of 400°C during 8 hours, the quantity of oxygen

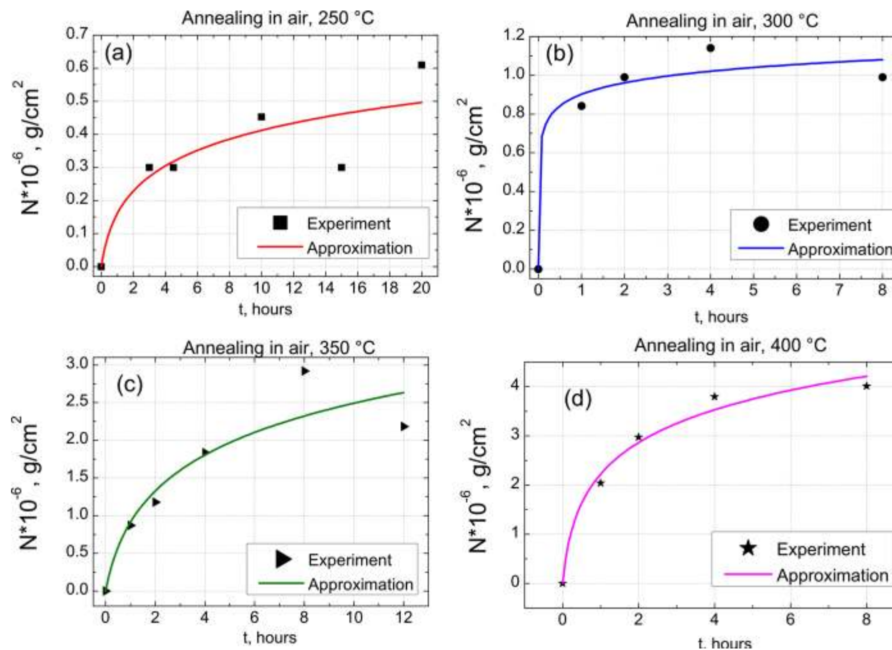

FIG. 10. Dependence of the quantity of oxygen in the oxide layer on the annealing time at different temperatures: (a) 250°C, (b) 300°C, (c) 350°C and (d) 400°C. The thin line is the logarithmic approximation from Eq. (2). The points are the results of experiment.

in the film was estimated to be 4.2×10^{-6} g/cm^2, which corresponds to an "effective" oxide layer of about 42 nm. This value is approximately 1.3 - 1.5 times higher than the SIMS data, which can be explained by the greater "effective" oxygen density in oxide films. Thus, the proposed model allows for the determination of the absolute quantity of oxygen in the Mo/Be MLM with reliable accuracy within 30 – 50 %.

Oxidation kinetics

It was shown in Ref. 23 that the dependence of the oxide layer thickness (or quantity of oxygen in the oxide layer) on anneal time can be described either by a logarithmic, a power-law dependence, or a parabolic dependence (Wagner's theory, Ref. 23) in specific physical cases. With a logarithmic dependence, the thickness of the oxide layer is small and the permeability of the layer is determined by the tunneling of electrons through the oxide layer (see a detailed discussion of the problem in Ref. 20). The important aspects are the crystalline structure and the temperature of the sample: for each type of structure and for each temperature, there exists a certain value of the oxide layer thickness for which further oxygen diffusion practically stops.

In the case of a power-law dependence, the growth rate of the oxide layer is determined by the rate of diffusion of oxygen ions within the oxide layer caused by a gradient of the oxygen ion concentration. The electrostatic field applied to the dielectric oxide film can influence this process.[20,23] The oxidation of metals in this case can be represented as an electrochemical process, leading to the creation of a potential difference between opposite sides of the oxide film. In the limit of thick oxide layers, this dependence becomes parabolic. For layers of moderate thickness, there will be a dependence on the exponent, i.e. quadratic and cubic, or some intermediate.

The experimental data was interpolated in Fig. 10 using a logarithmic dependence of the form:

$$N = k \times \ln(t/t_0 + 1) \tag{2}$$

where N is the quantity of oxygen atoms in the oxide layer, k is the constant of the logarithmic rate of increase in the quantity of oxygen, t is the annealing time and t_0 is the characteristic oxidation time.

It can be seen that the rate of growth of the oxide layer follows a logarithmic dependence. Consequently, each annealing temperature corresponds to a certain thickness of stable oxide layer formed at the surface. This also means that the moment the sample first comes into contact with oxygen, a fast and intensive oxidation of the surface occurs and the thickness of the oxide layer is determined by the temperature of the sample.

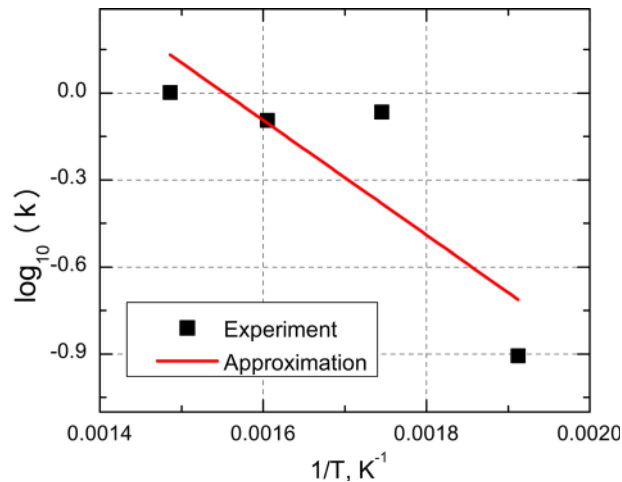

FIG. 11. Arrhenius dependence in coordinates $\log_{10}(k)$ vs 1/T. The slope of the fitted function corresponds to the activation energy of the oxidation process, determined to be 38 kJ/mol.

The activation energy of oxidation

In accordance with the Arrhenius equation, the rate of growth of the oxide film can be described by a dependence of the form:

$$k = \kappa_0 \times \exp(\frac{-Q}{R \times T}), \quad (3)$$

where k is the same constant of the logarithmic rate of increase in the quantity of oxygen as in Eq. (2), Q is the activation energy for the process, R is the gas constant, T is the thermodynamic temperature and κ_0 is the asymptotic oxidation speed at high temperatures.

The activation energy of the oxidation process was extracted from the slope of the Arrhenius plot, illustrated in Fig. 11, as 38 kJ/mol. This value coincides in order of magnitude with the activation energy for other oxidation processes in thin films.[20,24]

SUMMARY

The presented study of the oxidation processes and effects of annealing on structural and reflective properties of Mo/Be MLMs revealed a number of conclusions.

First, the Mo/Be system has a high structural stability, which is not typical for purely metallic MLMs. The small decrease in period (less than 0.5%) and widening of interlayer areas were observed starting from temperatures as high as 350°C. The inter-diffusion processes at the boundaries between the two layers are responsible for these transformations. The change of the transition region profiles from an error function to more a more linear behavior, which is typical for systems with a strong intermixing, indirectly supports this conclusion.

Second, it was shown that the main factor responsible for the observed decrease in EUV reflectance of an annealed Mo/Be MLM is the oxidation process occurring within the near-surface region. In the case of annealing in air atmosphere, the formation of the surface oxide layer is already starting at a temperature of 200°C. The samples annealed in a vacuum (residual pressure on the order of 1×10^{-4} Pa) withstand higher temperatures of up to 400°C.

Third, a slight increase of about 2%, which is comparable to the measurement error, was observed in the EUV peak reflectance of the sample annealed in vacuum at 300°C. This increase is hypothesized to be due to diffusion of oxygen atoms, absorbed mainly in Be layers of as-deposited samples, into the Mo layers. This redistribution leads to a decrease in the absorption of the standing wave in the MLM.

Fourth, a simple technique was developed which allows for the determination of the quantity of oxygen in the near-surface region of multilayers. This technique resulted in a quantification of the absolute quantity of oxygen in the MLMs as a function of annealing temperature and time. For instance, for the Mo/Be sample annealed at 400°C in air for 8 hours, the quantity of oxygen was estimated to be 4.2×10^{-6} g/cm^2, which corresponds to a 42 nm thick oxide layer assuming an oxygen density of 1 g/cm^2.

Fifth, it was established that the quantity of oxygen in the oxide layer grows logarithmically and reaches saturation at a certain thickness. The activation energy of the oxidation processes in the Mo/Be multilayer was determined to be about 38 kJ/mol.

Finally, it can be concluded that the results of this study give valuable information on the thermal stability and lifetime of Mo/Be multilayers, which is of practical interest for EUV lithography, solar imaging and other applications using the EUV reflecting coatings operating in conditions of high thermal load.

ACKNOWLEDGMENTS

This work was supported by the Russian Foundation for Basic Research (RFBR) [grant # 17–52–150006] for the sputtering, and the Russian Scientific Foundation [grant #RSF–DFG 16–42–01034] for the investigation of the structural parameters of the experimental samples, and RSF #17–12–01227 for the study of the reflectivity in the EUV range and annealing of the samples.

[1] N. I. Chkhalo, D. E. Pariev, V. N. Polkovnikov, N. N. Salashchenko, R. A. Shaposhnikov, I. L. Stroulea, M. V. Svechnikov, Yu. A. Vainer, and S. Yu. Zuev, "Be/Al-based multilayer mirrors with improved reflection and spectral selectivity for solar astronomy above 17 nm wavelength," Thin Solid Films **631**, 106–111 (2017).
[2] S. A. Bogachev, N. I. Chkhalo, S. V. Kuzin, D. E. Pariev, V. N. Polkovnikov, N. N. Salashchenko, S. V. Shestov, and S. Y. Zuev, "Advanced materials for multilayer mirrors for extreme ultraviolet solar astronomy," Applied Optics **55**, 2126–2135 (2016).
[3] S. Bajt, "Molybdenum–ruthenium/beryllium multilayer coatings," Journal of Vacuum Science & Technology A: Vacuum, Surfaces, and Films **18**, 557 (2000).
[4] K. M. Skulina, C. S. Alford, R. M. Bionta, D. M. Makowiecki, E. M. Gullikson, R. Soufli, J. B. Kortright, and J. H. Underwood, "Molybdenum/beryllium multilayer mirrors for normal incidence in the extreme ultraviolet," Applied Optics **34**, 3727–3730 (1995).
[5] A. E. Yakshin, R. W. E. van de Kruijs, I. Nedelcu, E. Zoethout, E. Louis, F. Bijkerk, H. Enkisch, and S. Müllender, "Enhanced reflectance of interface engineered Mo/Si multilayers produced by thermal particle deposition," Proc. SPIE **6517**, 65170I (2007).
[6] N. I. Chkhalo and N. N. Salashchenko, "Next generation nanolithography based on Ru/Be and Rh/Sr multilayer optics," AIP Advances **8**, 082130 (2013).
[7] N. I. Chkhalo, I. V. Malyshev, A. E. Pestov, V. N. Polkovnikov, N. N. Salashchenko, M. N. Toropov, and A. A. Soloviev, "Problems in the application of null lens for precise measurements of aspheric mirrors," Applied Optics **55**, 619–625 (2016).
[8] D. Brouns, A. Bendiksen, P. Broman, E. Casimiri, P. Colsters, P. Delmastro, D. de Graaf, P. Janssen, M. van de Kerkhof, R. Kramer, M. Kruizinga, H. Kuntzel, F. van der Meulen, D. Ockwell, M. Peter, D. Smith, B. Verbrugge, D. van de Weg, J. Wiley, N. Wojewoda, C. Zoldesi, and P. van Zwol, "NXE Pellicle: Offering a EUV pellicle solution to the industry," Proc. SPIE **9776**, 97761Y (2015).
[9] N. Chkhalo, S. Gusev, A. Nechay, D. Pariev, V. Polkovnikov, N. Salashchenko, F. Schäfers, M. Sertsu, A. Sokolov, M. Svechnikov, and D. Tatarsky, "High reflective Mo/Be/Si multilayers for the EUV lithography," Optics Letters **42**(24), 5070–5073 (2017).
[10] M. Svechnikov, D. Pariev, A. Nechay, N. Salashchenko, N. Chkhalo, Y. Vainer, and D. Gaman, "Extended model for the reconstruction of periodic multilayers from extreme ultraviolet and x-ray reflectivity data," Journal of Applied Crystallography **50**, 1428–1440 (2017).
[11] D. L. Windt, "IMD—Software for modeling the optical properties of multilayer films," Computers in Physics **12**, 360 (1998).
[12] M. S. Bibishkin, D. P. Chekhonadskih, N. I. Chkhalo, E. B. Klyuenkov, A. E. Pestov, N. N. Salashchenko, L. A. Shmaenok, I. G. Zabrodin, and S. Yu. Zuev, "Laboratory methods for investigations of multilayer mirrors in extreme ultraviolet and soft x-ray region," Proc. SPIE **5401**, 8–15 (2004).
[13] M. N. Drozdov, Y. N. Drozdov, N. I. Chkhalo, V. N. Polkovnikov, N. N. Salashchenko, P. A. Yunin, V. V. Roddatis, and A. Tolstogouzov, "The role of ultra-thin carbon barrier layers for fabrication of La/B_4C interferential mirrors: Study by time-of-flight secondary ion mass spectrometry and high-resolution transmission electron microscopy," Thin Solid Films **577**, 11–16 (2015).
[14] V. A. Chernov, N. I. Chkhalo, M. V. Fedorchenko, E. P. Kruglyakov, S. V. Mytnichenko, and S. G. Nikitenko, "Structural changes study of Co/C and Ni/C multilayers upon annealing," Journal of X-Ray Science and Technology **5**, 389–395 (1995).
[15] S. S. Andreev, M. M. Barysheva, N. I. Chkhalo, S. A. Gusev, A. E. Pestov, V. N. Polkovnikov, N. N. Salashchenko, L. A. Shmaenok, Yu. A. Vainer, and S. Yu. Zuev, "Multilayered mirrors based on La/B4C(B9C) for x-ray range near anomalous dispersion of boron (λ≈6.7nm)," Nuclear Instruments and Methods in Physics Research A **603**(1-2), 80–82 (2009).
[16] D. S. Kuznetsov, A. E. Yakshin, J. M. Sturm, R. W. E. van de Kruijs, E. Louis, and F. Bijkerk, "High-reflectance La/B-based multilayer mirror for 6x nm wavelength," Optics Letters **40**(16), 3778 (2015).
[17] I. A. Makhotkin, E. Zoethout, R. van de Kruijs, S. N. Yakunin, E. Louis, A. M. Yakunin, V. Banine, S. Müllender, and F. Bijkerk, "Short period La/B and LaN/B multilayer mirrors for ~6.8 nm wavelength," Optics Express **21**, 29894–29904 (2013).
[18] A. Galtayries, M.-H. Hu, K. Le Guen, J.-M. Andre, P. Jonnard, E. Meltchakov, C. Hecquet, and F. Delmotte, "Nanometer-designed Al/SiC periodic multilayers: Characterization by a multi-technique approach," Surface and Interface Analysis **42**, 653–657 (2010).
[19] H. Maury, J.-M. Andre, K. Le Guen, N. Mahne, A. Giglia, S. Nannarone, F. Bridou, F. Delmotte, and P. Jonnard, "Analysis of periodic Mo/Si multilayers: Influence of the Mo thickness," Surface Science **603**, 407–411 (2009).
[20] P. Kofstad, *High-Temperature Oxidation of Metals* (Wiley, New York, 1966).
[21] N. I. Chkhalo, M. N. Drozdov, E. B. Kluenkov, Ya. Al Lopatin, V. I. Luchin, N. N. Salashchenko, N. N. Tsybin, L. A. Sjmaenok, V. E. Banine, and A. M. Yakunin, "Free-standing spectral purity filters for extreme ultraviolet lithography," J. Micro/Nanolith. MEMS MOEMS **11**, 021115 (2012).
[22] B. L. Henke, E. M. Gullikson, and J. C. Davis, "X-ray interactions: Photoabsorption, scattering, transmission, and reflection at E = 50-30,000 eV, Z = 1-92," Atomic Data and Nuclear Data Tables **54**, 181–342 (1993).
[23] W. E. Garner, *Chemistry of the Solid State* (Academic Press, Inc., New York, 1955).
[24] T. Kacsich, K. P. Lieb, A. Schaper, and O. Schulte, "Oxidation of thin chromium nitride films: Kinetics and morphology," Journal of Physics: Condensed Matter **8**, 10703–10719 (1996).